



An energy-balance hydrologic model for the Lake Malawi Rift Basin, East Africa

Robert P. Lyons^{a,*}, Charles N. Kroll^b, Christopher A. Scholz^a

^a Department of Earth Sciences, Syracuse University, 204 Heroy Geology Laboratory, Syracuse, NY, 13244, USA

^b Department of Environmental Resources Engineering, SUNY ESF, 402 Baker Laboratory, Syracuse, NY, 13210, USA

ARTICLE INFO

Article history:

Received 6 May 2010

Accepted 20 October 2010

Available online 27 October 2010

Keywords:

Lake Malawi
hydrologic modeling
paleoclimate
lake-level

ABSTRACT

An energy-balanced hydrologic model is used to quantitatively assess atmosphere–water budget relationships across the Lake Malawi catchment, a hydrologically-open lake within the East African Rift System. The model first simulates the historical lake-level record over the last 100 years using climate station and vegetation data as inputs. Atmospheric conditions required to sustain equilibrium water balance are then estimated at known critical lake-levels: modern (700 m maximum water depth), basin closure (696 m maximum water depth), 500 m, 350 m, 200 m, and 150 m maximum water depth. The critical low lake stages were determined from analysis of seismic-reflection and deep lake drill-core data. The model predicts modern precipitation rate to be 955 mm/yr, which is consistent with observed climate station precipitation records. The minimum lowstand observed in geophysical records is 150 m water depth (550 m below present lake-level), and occurred about 95,000 years before present. The precipitation rate required to sustain equilibrium conditions at this low lake stage is 557 mm/yr, assuming modern Lake Malawi temperature and vegetation, and 374 mm/yr using modern temperature and vegetation data from the Little Karoo Basin, an analogue for the Malawi paleo-environment during severe arid intervals that resulted in major lake lowstands. The latter result is consistent with the range of precipitation measured from the Little Karoo Basin (100 to 500 mm/yr), and from interpretations of drill-core data sets (Cohen et al., 2007). The time required to drop lake-level from its modern maximum to the most severe low lake stage determined from paleoclimate data sets (from 700 m to 150 m maximum water depth) is less than 2500 years, even when accounting for additional water volume loss stored as groundwater. A lake-level fall of this magnitude reduces the lake surface area by 94% and reduces the total lake volume by 99%.

© 2010 Elsevier B.V. All rights reserved.

1. Introduction

Climate in the tropics is primarily controlled by effective moisture variability as a function of the change in position of the Intertropical Convergence Zone (ITCZ), which is one of the major drivers of tropical monsoon systems. As a result of high evaporation rates in addition to ITCZ migration, the hydrologic budgets and water levels of tropical lake basins are highly sensitive to their evaporation–precipitation water balances. However, there is a need for a quantitative understanding of the response of such lake water budgets to atmospheric variability. Tropical lake-levels can vary dramatically over times scales ranging from seasonal (e.g. Vollmer et al., 2005; Vallet-Coloumb et al., 2008), to historical (e.g. Drayton, 1984; Yin and Nicholson, 1998; Shanahan et al., 2007) to millennial (e.g. Russell and Johnson, 2007; Conroy et al., 2008; Shanahan et al., 2009), and most dramatically, over orbital times scales (e.g. D'Agostino et al., 2002; Scholz et al., 2003; Trauth et al., 2003; Brooks et al., 2005; McGlue et al., 2006; Anselmetti et al., 2009). The great lakes of East Africa,

including Lake Malawi, are no exception to this sensitivity (Lyons et al., 2009).

Large magnitude lake-level changes in Malawi are well-documented over both historical and orbital time scales. Over the last 100 years, lake-levels have dropped below the lake's outflow, causing complete hydrologic closure (Drayton, 1984), and Owen et al. (1990 and references therein) documented oral accounts of drought and low lake stages of as much as 40 m below present lake-level (BPLL) during the early 19th century. Over orbital time scales, seismic-reflection profiles and drill-core data sets document lake-level lowstands as much as 550 m BPLL (Scholz et al., 2007; Lyons et al., 2009). From analysis of scientific drill-core samples, it is also possible to extract paleo-environmental information such as vegetation and temperature (e.g. Beuning et al., 2010; Woltering et al., in press).

A new hydrologic model for the Lake Malawi drainage system provides insight into tropical hydrologic dynamics via atmosphere–lake water budget relationships, where key paleo-environmental parameters determined from drill-core data provide boundary conditions for lake-level simulations. Hydrologic modeling also permits estimates of the climate forcing necessary to induce large magnitude lake-level changes, and provides a better understanding of the potential impact of future climate change on this basin and the ecosystem as a whole.

* Corresponding author. Now at Chevron, 1400 Smith St. 29127 Houston, TX 77002, USA.
E-mail address: rplyons@syr.edu (R.P. Lyons).

Lake water budget models have helped assess the causative mechanisms behind large magnitude lake-level changes in a variety of tropical lacustrine basin settings. In South America, [Blodgett et al. \(1997\)](#) examined the climate conditions required to form and expand paleo-lakes in the Central Andes, by estimating evaporation through simultaneously solving the energy-balance equations and the bulk transfer formula for evaporation ([Brutsaert, 1982](#)). [Bookhagen et al. \(2001\)](#) modeled the conditions required to form a landslide-dammed lake in northwest Argentina ~30 000 ¹⁴C yr BP. In Lake Titicaca, [Rowe and Dunbar \(2004\)](#) modeled several lake stages using an energy-balance model, including paleo-lowstands documented from seismic-reflection profiles and sediment cores ([D'Agostino et al., 2002](#)).

In East Africa, Lake Tanganyika lowstands were modeled by [Bergonzini et al. \(1997\)](#) using an energy-balance model. [Bergner et al. \(2003\)](#) investigated the paleo-environmental conditions required for Lake Naivasha high lake stages also using an energy-balance model. In Malawi, [Owen et al. \(1990\)](#) calculated the lake's response time using simple water balance calculations and the lake's hypsometry to determine if rapid, large magnitude lake-level drops are feasible. [Calder et al. \(1995\)](#) and [Shanahan et al. \(2007\)](#) simulated historical lake-level records in Lake Malawi and West African Lake Bosumtwi, respectively, using a variety of modeling techniques.

Several of these studies used steady-state models, but did not consider transient non-equilibrium conditions, specifically those that occur on a sub-annual basis. Therefore, they could not consider seasonal variability of precipitation, and thus only calculated potential evaporation on land and not actual catchment water loss due to evaporation. This process can be especially important during dry seasons in tropical settings when precipitation is negligible for several months. The few transient models ([Calder et al., 1995](#); [Shanahan et al., 2007](#)) only simulated the historical lake-level records, and did not evaluate ancient systems over geological time frames where the amplitude of lake-level change can be much higher. Several studies considered lake response times (e.g. [Bookhagen et al., 2001](#); [Bergner et al., 2003](#); [Rowe and Dunbar, 2004](#)), but none considered the effect of additional volume stored as groundwater as lake-levels changed.

This study presents a transient, energy-balance hydrologic model that simulates the last 100 years of Malawi lake-level over monthly time steps. Using model output values from both modern and lowstand analogue evaporation scenarios, we estimate the precipitation rate required to sustain equilibrium conditions at low lake stages. Finally, we determine Lake Malawi's time-depth response from induced precipitation and evaporation change.

2. Regional setting

2.1. Geologic setting

Lake Malawi is located at the southern end of the East African Rift System between 9° and 15° S ([Fig. 1](#)). The rift valley is nearly completely covered by the lake, and is structurally controlled by a series of alternating half-graben basins where basin-bounding faults have displacements of 5 km or more, and uplifted rift flanks extend more than 1000 m above the modern lake surface ([Specht and Rosendahl, 1989](#)).

The geology of the region consists of Precambrian metamorphic basement rocks overlain by Permo-Triassic and Mesozoic sedimentary rocks ([Malawi Department of Surveys, 1983](#); [Mozambique Ministry of Mineral Resources, 1987](#)). Crystalline Precambrian basement rocks are exposed throughout the catchment, and thick Quaternary deposits are observed adjacent to the lake coastlines and within the lake. The very low permeability Precambrian crystalline rocks surrounding the lake basin limit groundwater infiltration into the lake ([Smith-Carrington and Chilton, 1983](#); [Owen et al., 1990](#)).

2.2. Modern climate and hydrology

The climate in the region is controlled by the annual migration of the Intertropical Convergence Zone (ITCZ), bringing a single wet season during the austral summer (November–April) ([Malawi Department of Surveys, 1983](#)) ([Figs. 2 and 3](#)). This wet season produces nearly all the rainfall observed in the Lake Malawi drainage system. The dry season during the austral winter (June–August) produces almost no rain ([Figs. 2 and 3](#)), so that many of the smaller streams in the catchment are ephemeral systems and the larger river systems produce highly variable outflow depending on the season ([Kingdon et al., 1999](#)). The mean annual temperature for the basin is 22.4 °C over land and 24.8 °C over water (from 1992–2007 averages of climate station data).

Lake Malawi hypsometry and cumulative water volume were determined from interpretations of seismic-reflection profiles ([Fig. 4](#)). Due to rapid fault-related subsidence and a climate favoring a positive water balance, Lake Malawi is the 4th largest lake in the world by volume (7720 km³). Presently the lake is a maximum of 700 m-deep, 580 km long, and up to 80 km wide, with a surface area of 29,400 km² ([Fig. 4](#)) and catchment area of 128,000 km².

Several large river drainage systems are present throughout the watershed, almost all of which enter the lake from the west ([Kingdon et al., 1999](#)) ([Fig. 1](#)). The Ruhuhu River system is the only major drainage system that enters on the eastern shore ([Fig. 1](#)), but it contributes the highest amount of annual inflow (20%) to the lake ([Kidd, 1983](#); [Kingdon et al., 1999](#)). All other major rivers individually contribute less than 10% of the total annual inflow to the lake ([Kidd, 1983](#); [Kingdon et al., 1999](#)). The Shire River is the lake's sole outlet, with a relatively small but highly variable annual discharge that is a function of lake-level ([Drayton, 1984](#)). The elevation of the sill (Shire River bottom) is 471 m above sea level (masl) and modern lake-level is 475 masl. Although at 4 m today, the sill depth has varied dramatically even over historical time scales ([Drayton, 1984](#)) ([Fig. 5](#)).

Water storage in Lake Malawi is primarily governed by its precipitation-evaporation balance. Annual precipitation varies spatially throughout the basin, ranging from <800 mm/yr on the southern lake shore to >2400 mm/yr in the northern highland areas ([Malawi Department of Surveys, 1983](#)). This is due to a variety of factors, including elevation and rain-shadow effects, convergence due to prevailing winds, and proximity to the lake shore. Water balance studies have documented annual evaporation values ranging between 1000 and 1400 mm/yr ([Kidd, 1983](#); [Owen et al., 1990](#)). The high precipitation and evaporation, coupled with limited groundwater inflow and low annual outflow, results in seasonal lake-level variations of up to 2 m ([Fig. 5](#)).

The historical lake-level record demonstrates the sensitivity of this tropical rift basin to changes in the hydrologic cycle ([Fig. 5](#)). In 1915, lake-level dropped below the sill elevation of the Shire River to almost 470 masl, successfully closing the basin. Since the outflow accounts for the only direct loss from the lake other than evaporation, hydrologically closing the basin increases the sensitivity of the lake to further climate change. [Owen et al. \(1990, and references therein\)](#) documented Lake Malawi lowstands as low as 40 m below present lake-levels (BPLL) in the 19th century and explain potential lake-level drops of nearly 150 m between A.D. 1390 and A.D. 1860.

2.3. Evidence for ancient lake lowstands

Several studies document that the lake has experienced extreme low lake-levels in the past. The best evidence for these large events comes from multiple vintages of seismic-reflection data and from well-dated drill-core data from the Lake Malawi Drilling Project ([Scholz et al., 2007](#); [Lyons et al., 2009](#)). Based on seismic-reflection profiles, several authors document the presence of lowstand delta

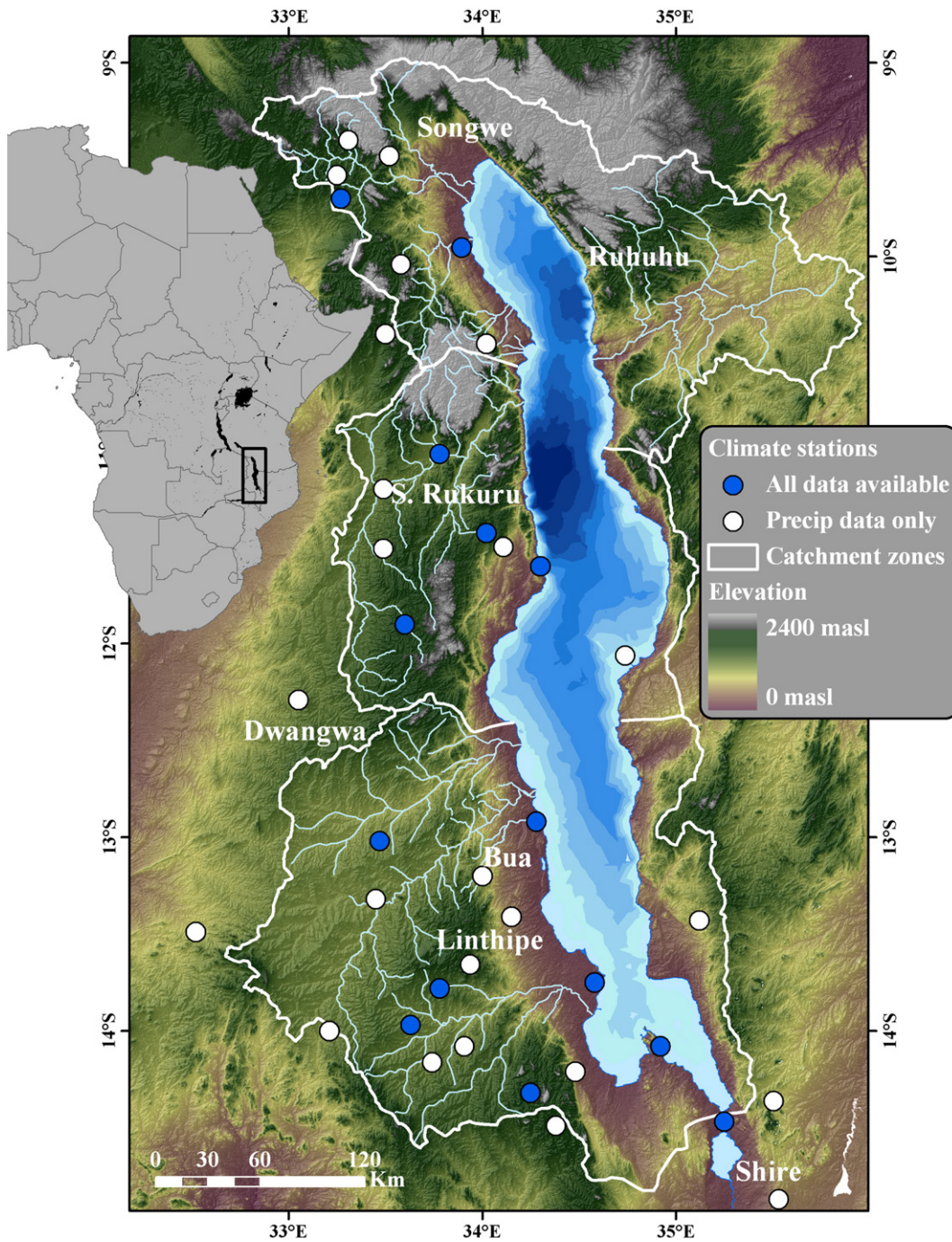


Fig. 1. Hill-shaded Satellite Radar Topography Mission (SRTM) 30-m resolution digital elevation model of the Lake Malawi catchment. The three catchment zones used to estimate the basin-averaged precipitation rate are outlined in white (following Kidd, 1983). Of the 47 available climate stations, 38 were in the Lake Malawi catchment. Of those 38, 24 have only precipitation data available (white), and 14 have both precipitation and evaporation data available (blue).

deposits up to 500 m below present lake-level, and erosional truncation surfaces 550 m BPLL (Martin, 1997; Soreghan et al., 1999; Buoniconti, 2000; Lyons et al., 2009). Each delta downlap surface (200, 350, and 500 m BPLL) and erosional truncation surface (up to 550 m BPLL) has been successfully correlated to the drill site locations, where geochemical and geophysical evidence suggests that lowstands occurred during solar insolation minima when carbonate-rich, organic-poor, high-density sediments accumulated (Scholz et al., 2007; Cohen et al., 2007; Lyons et al., 2009). Each major lowstand was preceded and followed by highstand conditions (during insolation maxima) that were comparable to the modern,

700 m-deep lake stage. Paleobiological and paleoecological data from the drill-core suggests that the lake was alkaline and mildly saline during the dry episodes, and that the location of the drill site may have briefly been within 5 m of the paleo-shoreline (Cohen et al., 2007; Beuning et al., 2010). During these arid periods the catchment had widespread semi-desert environments around the lakeshore areas, and extensive coniferous (*Podocarpus*-dominate) forest in the highlands (Cohen et al., 2007; Beuning et al., 2010). In this paper, we discuss these major low stages documented in the drill-core and seismic-reflection studies in terms of their paleo-maximum water depths.

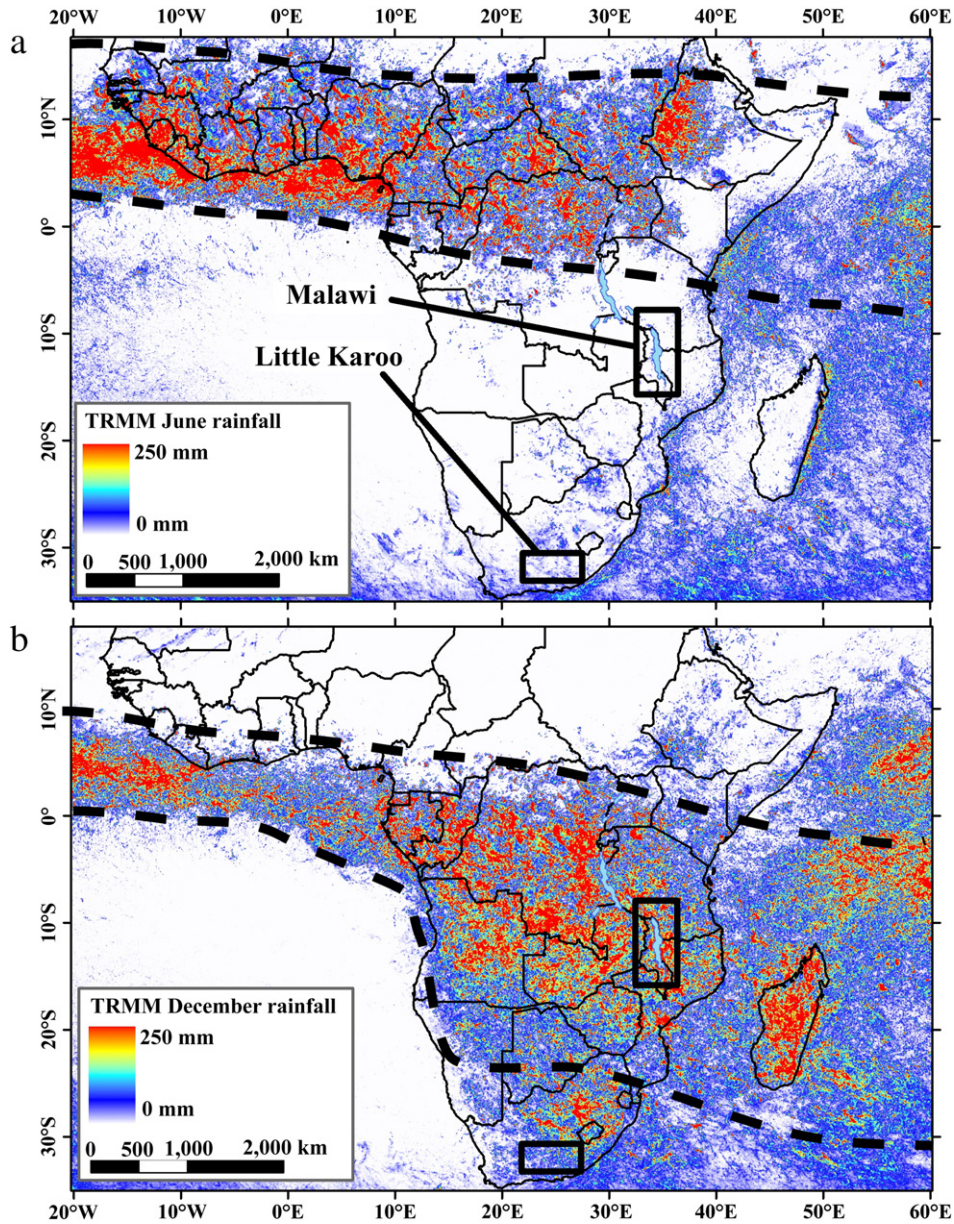


Fig. 2. African mean total monthly rainfall from 1997 to 2006 using the TRMM2b-31 (combined TMI and PR) data for June (a) and December (b) (Mulligan, M, 2006, Global Gridded 1 km TRMM Rainfall Climatology and Derivatives, Version 1.0. Database: <http://www.ambiotek.com/1kmrainfall>). Approximate boundaries of the ITCZ are marked with dashed lines (adapted from Nicholson, 2000).

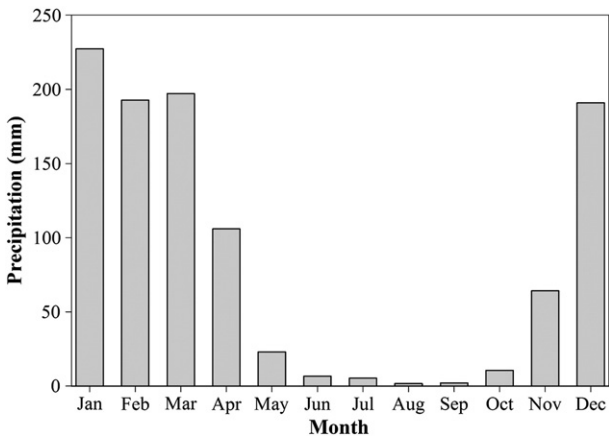


Fig. 3. Basin-averaged monthly precipitation rate from 1956 to 2008 over the entire Lake Malawi catchment.

3. Materials and methods

3.1. Water budget model

The water balance for Lake Malawi can be expressed as a balance between hydrologic inputs and outputs:

$$\Delta V = P - E_w - E_l - O - G \tag{1}$$

where ΔV is the change in lake volume, P is precipitation directly onto the lake or onto the surrounding land that is part of the catchment, E_w is evaporation from the lake, E_l is evaporation from the catchment, O is outflow (from the Shire River), and G is net groundwater outflow from the lake. Using hypsometric data from the lake basin, changes in total volume (from Eq. (1)) and lake surface area can be expressed in terms of changes in the elevation of the lake surface (Fig. 4). Lake Malawi water bottom morphology was assessed using more than 10,000 km of seismic-reflection profiles collected across the basin

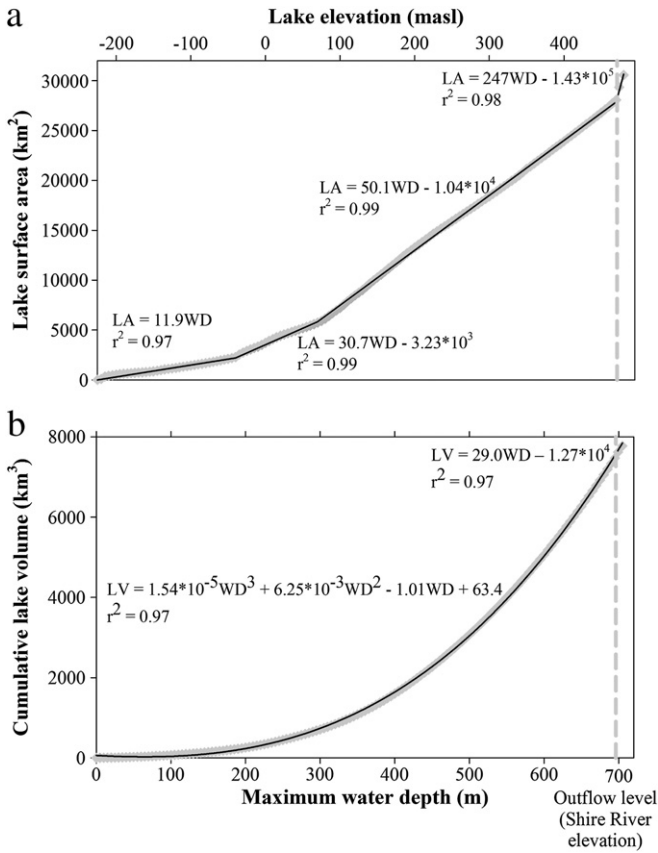


Fig. 4. Malawi bathymetric morphology. LA is lake area, LV is lake volume, and WD is water depth. (a) Lake hypsometry with equations used to define lake area change with depth. (b) Cumulative water volume with equations used to define volume change with water depth. Gray points are individual data points at each water depth and the lines are the least-squares fits describing the points.

(Lyons et al., 2009). Lake hypsometry is defined by a series of linear regressions (Fig. 4a) and cumulative volume is defined by a linear regression where maximum water depth is greater than 680 m, and a third-order polynomial where maximum water depth is less than 680 m (Fig. 4b).

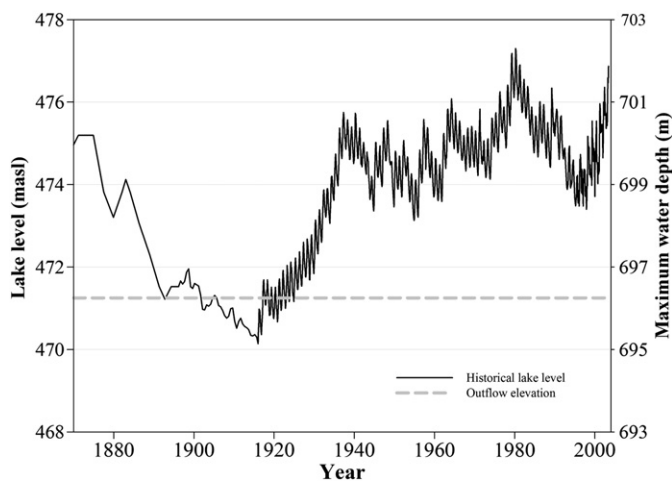


Fig. 5. Historical Malawi lake-level record. Before 1916 lake-level was only recorded every 1–3 years, whereas afterwards it was recorded every month. In 1915, lake-level dropped below the sill elevation of 696 masl, hydrologically closing the basin. Data after 1995 are from satellite radar altimetry, downloaded from the Global Reservoir and Lake Elevation Database (http://www.pecad.fas.usda.gov/cropexplorer/global_reservoir/).

3.2. Precipitation

Monthly climate data were acquired from the office of Malawi Meteorological Services, and included precipitation, air temperature, wind speed, relative humidity, and daily sunshine hours. The precipitation data set consists of monthly rainfall measurements from January 1903 to January 2008. Forty-seven stations are available, and 38 are within or in proximity to the lake's catchment (Fig. 1). The entire catchment was divided into three zones (following Kidd, 1983), and average precipitation from each zone was weighted by its area to determine the basin-averaged precipitation rate (P_{bas}) for the entire historical record (Fig. 1).

3.3. Evaporation

Evaporation was calculated separately over land and water and multiplied over each respective area. Lake surface area varies with changing lake-level, thereby changing the spatial extent of over land versus over water evaporation. The evaporation subcomponent of the energy-balance hydrologic model can be expressed by simultaneously solving the energy-balance equations for evaporation and the bulk transfer formula for evaporation (Brutsaert, 1982) to determine surface temperature (T_s) for both land and water (Blodgett et al., 1997) (Fig. 6, Table 1). Shanahan et al. (2007) demonstrated that this method performs as well if not better than several other commonly used evaporation models for simulating lake-level response in tropical lake settings. We also recognize that heat storage in the lake could be an important parameter for estimating evaporation under certain scenarios. While this topic justifies further research, it is beyond the scope of this paper.

Several evaporation model inputs are available since 1956 for a subset of the climate stations (Fig. 1), including air temperature, relative humidity, daily sunshine hours, and wind speed. Monthly values for relative humidity and number of sunshine hours were averaged for each year in the data set. The climate stations were subdivided into the shoreline stations and non-shoreline stations to determine air temperature over land and water separately. A single average value for wind speed (2.67 m/s) was used for the entire historical record. Varying air pressure as lake-level changed caused the model output for evaporation to vary by less than 10 mm/yr, so a single averaged value for air pressure was used in all simulations (Table 1). To estimate evaporation for the period prior to 1956, where no evaporation model inputs are available, monthly averages from the past 50 years were calculated for each input parameter (Table 1).

Four parameters in the evaporation model depend on vegetation type: albedo, surface emissivity, soil moisture, and the roughness length (Fig. 6, Tables 1 and 2). Vegetation type was determined from the Globcover data set provided by ESA and the ESA Globcover Project led by MEDIAS France (<http://postel.mediasfrance.org/>) (Fig. 7, Table 2). This 300-m resolution global land cover data set uses the FAO-UNEP Land Cover Classification System (LCCS: http://www.fao.org/sd/2001/EN0101_en.htm). The LCCS was reclassified into nine primary vegetation types (Table 2), and published values for the four vegetation parameters were used (Bougeault, 1991). Area-weighted values of each parameter were then calculated for input into the evaporation subcomponent of the model (Fig. 6, Tables 1 and 2).

3.4. Groundwater and outflow

The net change in groundwater for the water budget is assumed negligible, given that Precambrian gneissic basement rocks are predominant throughout the catchment, and are adjacent to the lake shoreline in the vicinity of high-angle border faults. For calculating outflow, the Shire River discharge-lake depth relationship determined by Drayton (1984) was used in the model. This

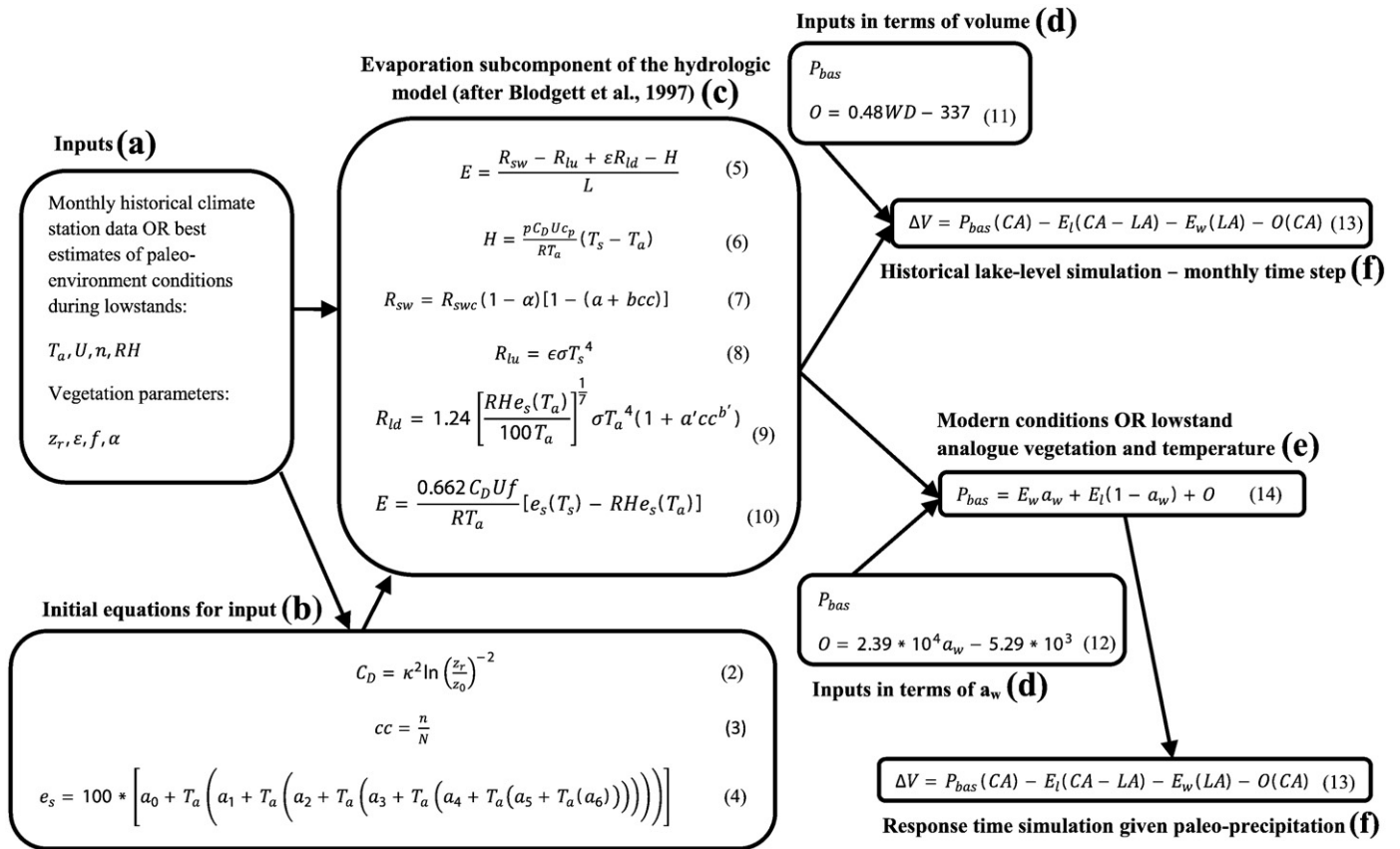


Fig. 6. Flow-chart of the modeling procedure used in this study. (a) Procedures regarding the generation of input parameters are described in the Methods section and listed in Table 1. (b) Equations used to calculate input parameters used in the evaporation subcomponent of the model. For Eq. (4), $a_0 = 6984.505294$, $a_1 = -188.9039310$, $a_2 = 2.133357675$, $a_3 = -1.288580973 * 10^{-2}$, $a_4 = 4.393587233 * 10^{-5}$, $a_5 = -8.023923082 * 10^{-8}$, $a_6 = 6.136820929 * 10^{-11}$ (Brutsaert, 1982; Table 1). (c) The evaporation subcomponent of the hydrologic model. (d) Inputs (outflow and basin-averaged precipitation) for lake area and volume calculations either on monthly or annual time steps for the historical simulation and response time simulations, respectively. (e) Equilibrium equations used to calculate the precipitation required to drop lake-level to a known critical magnitude (Tables 2 and 3). (f) Lake area and volume equations defined in Fig. 4 for both monthly and annual time steps.

relationship is presented in basin-equivalent values (mm/yr) by dividing the volumetric discharge measurements by the catchment area.

3.5. Historical lake-level simulation

To simulate the Malawi historical lake-level record, the energy-balance hydrologic model is used with a monthly time step (Blodgett et al., 1997) (Fig. 6, Table 1). Monthly steps are critical to the model's success because of the wet-dry seasonal cycle within the catchment (Figs. 2 and 3). During the dry season, precipitation is less than evaporation on land. The calculated evaporation on land is the potential evaporation, which assumes an infinite amount of water is available to evaporate. In this model, evaporation on land is set to be no more than the basin-averaged amount of precipitation for any given month. Over the lake, however, evaporation can be significantly greater than precipitation throughout the year. After the net change in storage in Lake Malawi is determined for a given month, resulting lake-level change is calculated using the cumulative volume and hypsometry functions (Fig. 4).

3.6. Low lake stage simulation

To investigate paleoclimatic conditions required to produce ancient lowstands in the lake, a steady-state lake water balance (Hastenrath and Kutzbach, 1983) is employed:

$$P_{bas} = E_w a_w + E_l(1 - a_w) + O \quad (14)$$

where P_{bas} is the basin-averaged precipitation rate, E_w is the evaporation rate over water, E_l is the evaporation rate over land, and a_w is the lake area-catchment area ratio (a function of lake-level) (Fig. 6). Given the evaporation rate and outflow, the precipitation rate required to sustain equilibrium can be determined at any lake stage. Using Eq. (14), two critical historical lake stages are assessed: 700 m, the modern lake-level; and 696 m, where the basin becomes closed. This is accomplished using modern values of evaporation over land and water, calculated from 1992–2007 averages of input parameters.

Two evaporation scenarios are used to determine the precipitation required to sustain equilibrium conditions during low lake stages: holding evaporation to modern conditions, and changing the evaporation rate by using a modern temperature and vegetation analogue to the ancient Malawi catchment (during lowstands). Cohen et al. (2007) and Beuning et al. (2010) suggested that lowstand paleo-environmental conditions around Lake Malawi were similar to the modern highlands of southern Africa, trending towards more semi-desert vegetation and cooler temperatures. These interpretations are based on paleoecological and paleoenvironmental indicators from well-dated discrete drill-core samples, such as pollen, ostracodes, diatoms, charred particle presence, and chaoborids. The modern South African Little Karoo Basin may approximate vegetation and temperature conditions that developed during the severe megadroughts postulated for the Malawi Rift Valley at 95 ka (Scholz et al., 2007; Cohen et al., 2007) (Fig. 8, Tables 1 and 2). Similar to the Malawi Basin, the Little Karoo catchment has considerable relief, with the basin floor at 300 masl, and the highlands at 1800 masl (Fig. 8), but the mean annual temperature for the Little Karoo Basin is 17.5 °C (5–7 °C cooler than Malawi) (Desmet and Cowling, 1999). Due to

Table 1
Input and output parameters from the evaporation subcomponent of the energy-balance hydrologic model.

Parameter	Description	Modern value (or 1992–2007 annual averages)	Best-estimate lowstand value	Units	Notes
T_a	Air temperature (w/l)	24.8/22.4	17.5/17.5	°C	Modern from climate stations / best estimate lowstand from Desmet and Cowling, 1999
U	Wind speed	2.67	2.67	m/s	Modern from climate stations
N	Maximum possible hours of sunshine	12.1	12.1	h	Modern from climate stations
n	Number of sunshine hours	7.82	7.82	h	Modern from climate stations
RH	Relative humidity	0.66	0.66	–	Modern from climate stations
z_r	Reference height (w / l)	2.0/130.0	2.0/130.0	M	From Bergner et al., 2003
z_0	Roughness length (w / l)	$1.0 * 10^{-4} / 0.35$	$1.0 * 10^{-4} / 0.27$	M	Calculated from Globcover data set
f	Soil moisture (w/l)	1.0/0.51	1.0/0.39	–	Calculated from Globcover data set
α	Albedo (w/l)	0.06/0.14	0.06/0.09	–	Calculated from Globcover data set
ϵ	Surface emissivity (w/l)	1.00/0.92	1.00/0.07	–	Calculated from Globcover data set
C_D	Surface drag coefficient (w/l)	$1.6 * 10^{-3} / 4.5 * 10^{-3}$	$1.6 * 10^{-3} / 4.2 * 10^{-3}$	–	Calculated according to Bookhagen et al., 2001
cc	Cloud cover	0.64	0.64	–	$cc = n/N$ where $N = 12.1$ h
$e_s(T_a)$	Saturation vapor pressure - air (w / l)	3147/2725	1998/1998	Pa	Calculated according to Brutsaert, 1982
$e_s(T_s)$	Saturation vapor pressure - surface (w / l)	3796/2923	2525/2391	Pa	Calculated according to Brutsaert, 1982
p	Air pressure	95803	95803	Pa	from average elevation of the catchment
c_p	Specific heat of dry air	1005	1005	J/K kg	Constant
R	Gas constant for dry air	287	287	J/K kg	Constant
σ	Stefan-Boltzmann constant	$5.6697 * 10^{-8}$	$5.6697 * 10^{-8}$	$m^{-2} K^{-4}$	Constant
k	von Karman constant	0.4	0.4	–	Constant
a	Shortwave cloud parameter	0.4	0.4	–	From Budyko, 1974
b	Shortwave cloud parameter	0.38	0.38	–	From Budyko, 1974
a'	Longwave cloud parameter	0.55	0.55	–	From Budyko, 1974
b'	Longwave cloud parameter	2.0	2.0	–	From Budyko, 1974
L	Latent heat of vaporization	$2.26 * 10^6$	$2.26 * 10^6$	J/kg	Constant
$R_{s_{wc}}$	Cloud-free shortwave radiation	410.9	410.9	W/m ²	From Laskar et al., 2004
R_{sw}	Net shortwave radiation (w/l)	137/126	137/132	W/m ²	Calculated using energy budget equations
R_{lu}	Longwave radiation up (w/l)	466/402	426/295	W/m ²	Calculated using energy budget equations
R_{ld}	Longwave radiation down (w/l)	465/442	397/397	W/m ²	Calculated using energy budget equations
H	Sensible heating rate (w/l)	15.5/16.3	19.2/37.7	W/m ²	Calculated using energy budget equations
T_s	Surface temperature (w/l)	27.9/23.5	21.3/20.4	°C	Calculated using energy budget equations
E_w/E_l	Evaporation (w/l)	1665/521	1218/362	mm/yr	Calculated using energy budget equations

a different climatic regime, the vegetation distribution of the Little Karoo Basin is markedly different than in the Malawi catchment (Fig. 8; Table 2). Malawi has 17% of its total land area covered by croplands, while the Little Karoo basin is 5% croplands. Whereas Malawi has a higher percentage of shrublands than Little Karoo (24% vs. 12%, respectively), Little Karoo has a markedly higher percentage of land area covered by grasslands (33% vs. 2%, respectively), a strong indicator of dryer conditions (Table 2). Malawi has a slightly higher percentage of woodlands (57% vs. 48%, respectively), and whereas the Little Karoo is 3% desert, the Lake Malawi catchment has no desert (Table 2). Using Eq. (14) and both the modern Malawi and Little Karoo evaporation scenarios, the basin-averaged precipitation rate required to sustain equilibrium water balance is determined for low lake stages in 50-m increments below the modern maximum water depth of 700 m (Table 3).

3.7. Response time estimation

To determine the response time of lake-level to climate change, paleo-precipitation estimates for critical low lake stages from the

lowstand simulations (Tables 1 and 2) are applied instantaneously to modern Malawi lake-level using the modern vegetation and temperature for the catchment (Fig. 8). Even though groundwater contribution on a semi-annual to annual basis is considered negligible, the volume lost or gained during lake-level fall or rise, respectively, must be accounted for when considering the response time of the hydrologic system over 100's to 1000's of years. Thus, time-depth curves in both the draw-down and refill directions are calculated on annual time steps using three scenarios. In Scenario 1, Lake Malawi is a no-flow boundary, and therefore there is no groundwater gain to, or loss from, the lake. Given that much of the Lake Malawi coastline is bounded by large-offset, high-angle normal faults, for Scenario 2 these faults are assumed to be vertical no-flow boundaries that intersect the Lake Malawi shoreline, and extend infinitely in the vertical direction (Fig. 9). As a result, water is potentially stored between the bottom of Lake Malawi and these vertical boundaries. A porosity value of 15% was used for this storage material, assuming a composite of alluvial sediments and sedimentary rocks (Schwartz and Zhang, 2002 and references therein). The water table elevation is assumed to be the same as the elevation of the lake. Thus as lake-level

Table 2
Globcover legend and environmental input parameters used for calculating evaporation on land.

Bougealt (1991) description	Albedo (%)	Surface emissivity	Soil moisture	Roughness length (cm)	Malawi distribution (%)	Little Karoo distribution (%)
Croplands	15	0.90	0.30	20.00	17.21	4.76
Woodlands	10	0.95	0.75	50.00	57.30	48.21
Shrublands	20	0.85	0.10	10.00	23.71	11.64
Grasslands	25	0.80	0.05	5.00	1.69	32.51
Aquatic	8	1.00	0.83	0.01	0.08	0.00
Desert	30	0.75	0.02	1.00	0.00	2.73
Salt hardpans	–	–	–	–	–	–
Water bodies	–	–	–	–	–	–
Permanent snow and ice	–	–	–	–	–	–
No data	–	–	–	–	–	–

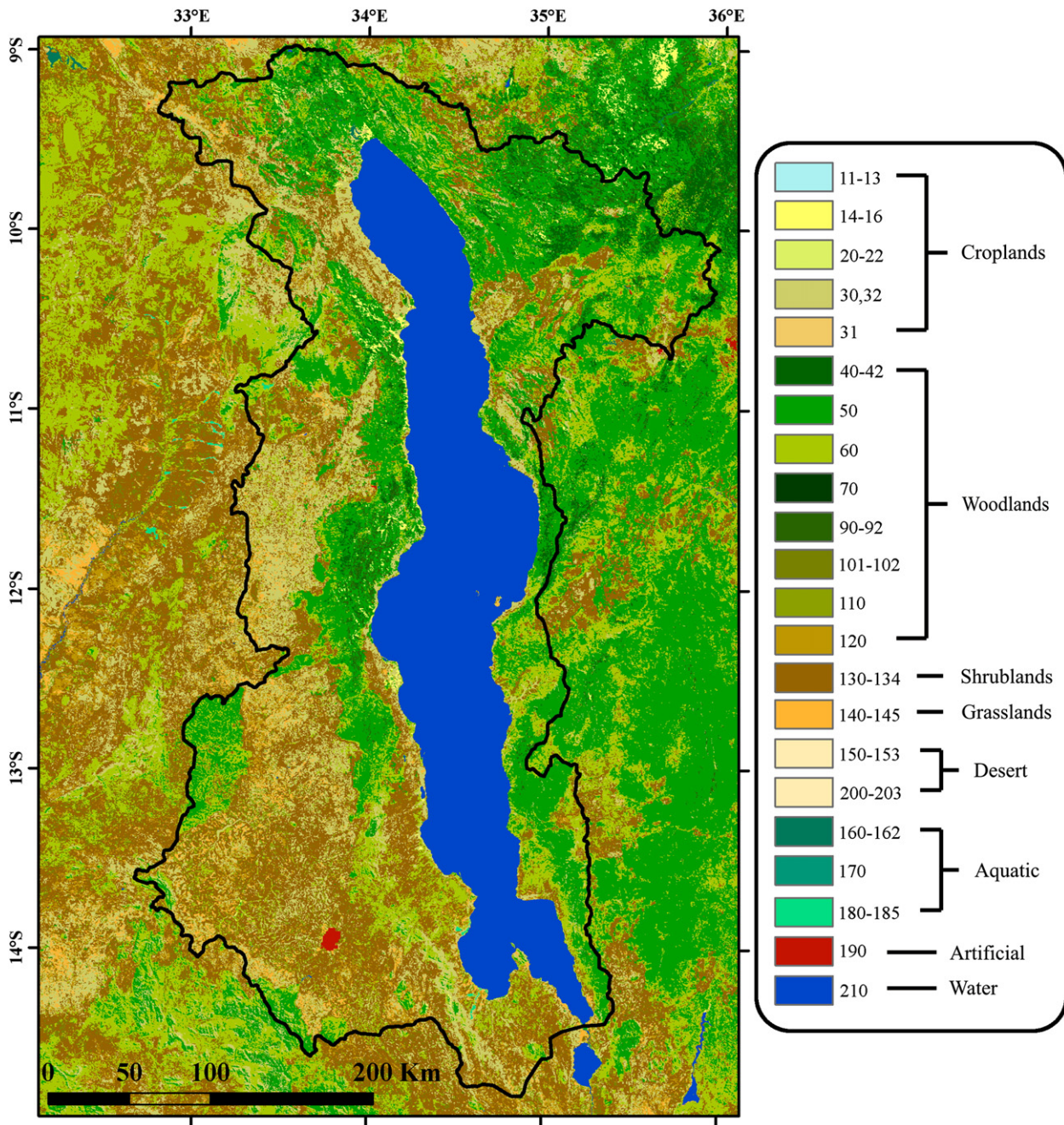


Fig. 7. Globcover vegetation map for the Lake Malawi catchment. Numbers in the legend indicate LCSS type (http://www.fao.org/sd/2001/EN0101_en.htm). Vegetation-dependent variables and distributions are presented in Table 2.

varies, so does the water table and therefore the amount of storage within the groundwater system. Knowledge of the total volume stored as groundwater is not required because only the change in the volume of groundwater stored as lake-level varies is of interest. In Scenario 3, the vertical no-flow boundaries are located farther from the modern Lake Malawi shoreline to include Quaternary alluvium and Tertiary sedimentary section that is connected to the lake shore (Fig. 9). This scenario is essentially the same as Scenario 2, except the boundaries are extended laterally away from the lake shore while still assuming 15% porosity of storage material.

Cumulative volume plots of the three scenarios demonstrate the effect of adding potential groundwater storage to the total volume of the reservoir (Fig. 10). When maximum depth increases, the total water volume in the reservoir increases exponentially. The Scenario 1 cumulative volume plot is the same shown in Fig. 4b. At each suc-

cessive elevation, scenarios 2 and 3 add an additional volume relative to Scenario 1.

4. Results

4.1. Historical lake-level simulation

The historical model simulates the lake-level record in Lake Malawi over the last 50 years reasonably well (Fig. 11). However, prior to 1950 the model does not perform as well, especially during the interval of lake-level rise between 1920 and 1950. This lack of agreement can be explained by two factors. First, data constraining parameters that contribute to the evaporation subcomponent of the model (Table 1) extend only from 1956 to today; for the earlier interval monthly averages of each transient evaporation input (air

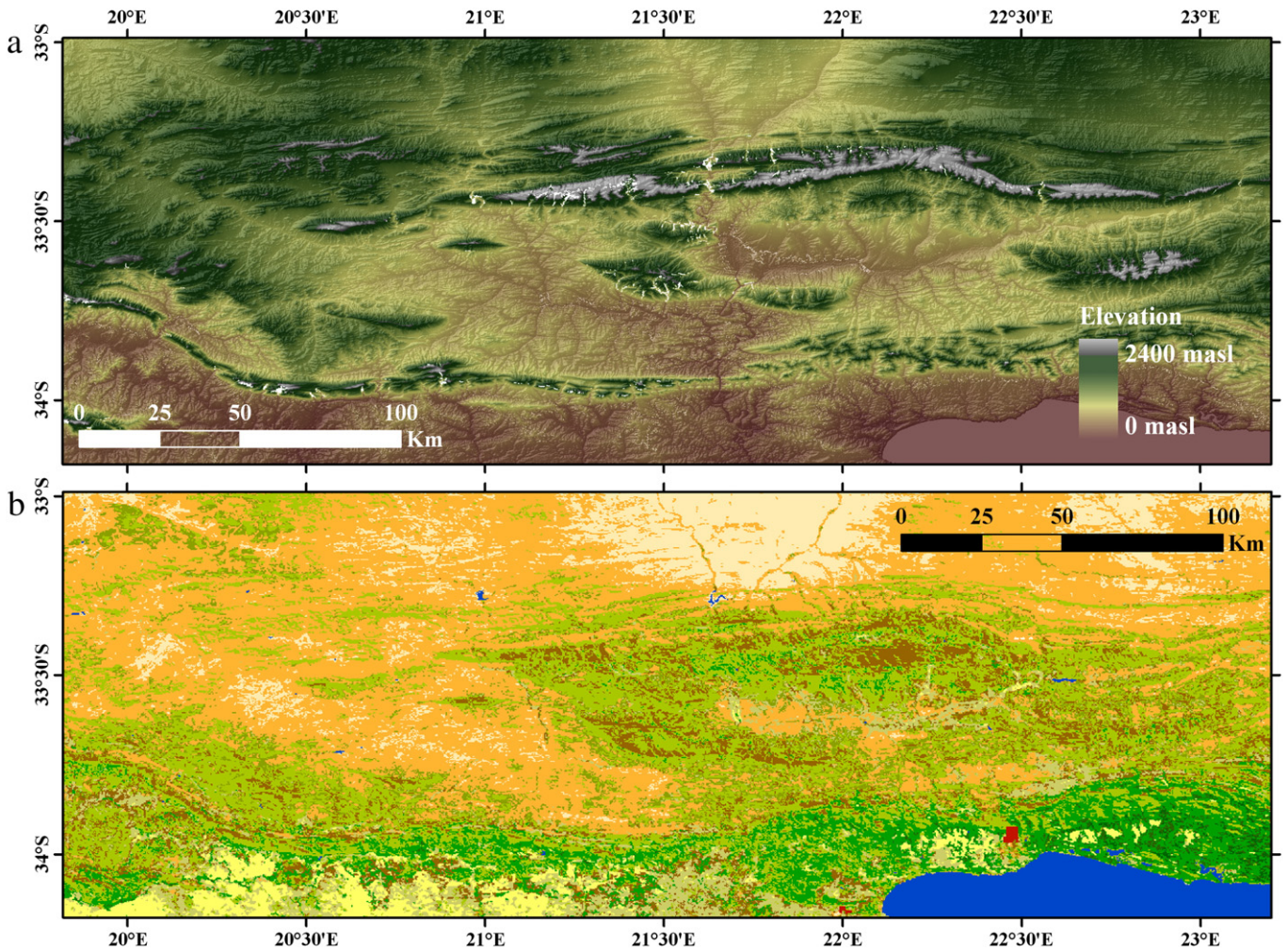


Fig. 8. (a) Hill-shaded SRTM 30-m resolution digital elevation model for the Little Karoo Basin. The elevation scale used here is the same as in Fig. 1. (b) Globcover data set for the Little Karoo Basin. The color scheme used here is the same used in Fig. 7. The more desert-like conditions relative to the Malawi Basin can be seen by an increased amount of beige colors. See Table 2 for classification routine.

temperature, relative humidity, and number of sunshine hours) were used. Accordingly the estimates of evaporation may be incorrect. Furthermore, precipitation data are limited in the early part of the historical record. Secondly, an underestimation of lake-levels between 1928 and 1948 may be due to the development of sand bars at the

mouth of the Shire River during a lowstand in 1915, when lake-level dropped below the outlet sill depth (Calder et al., 1995) (Fig. 5). During the transgression following this lowstand, a lake-level rise to an elevation greater than the elevation of the modern sill depth (471 masl) of the Shire River was required to breach sand bars that

Table 3
Lake surface areas and volumes at varying lake-levels.

Water depth – WD (m)	Elevation (masl)	Lake area – LA (*10 ³ km ²)	% Lake area	a _w	Total volume – V (*10 ³ km ³)	% Total volume
700 ^a	475	29.4	100.0	0.23	7.6	100.0
696.25 ^a	471.25	28.5	96.9	0.22	7.5	98.6
650	425	25.4	86.3	0.20	6.3	82.2
600	375	22.6	76.9	0.18	5.0	65.9
550	325	19.9	67.6	0.15	4.0	51.9
500 ^b	275	17.1	58.2	0.13	3.0	39.9
450	225	14.4	48.8	0.11	2.3	29.9
400	175	11.6	39.5	0.09	1.6	21.6
350 ^b	125	8.9	30.1	0.07	1.1	14.9
300	75	6.1	20.7	0.05	0.7	9.7
250	25	4.5	15.1	0.03	0.4	5.8
200 ^b	–25	2.9	9.9	0.02	0.2	3.1
150 ^b	–75	1.8	6.1	0.01	0.1	1.4
100 ^c	–125	1.2	4.0	0.01	0.04	0.5

a_w is lake area–catchment area ratio.

^a Critical lake-levels identified in the historical lake-level simulation.

^b Critical lake-levels identified from seismic-reflection profiles and dated from drill-core data (Scholz et al., 2007; Lyons et al., 2009).

^c Critical lake-level identified as a possible paleosol (Cohen et al., 2007).

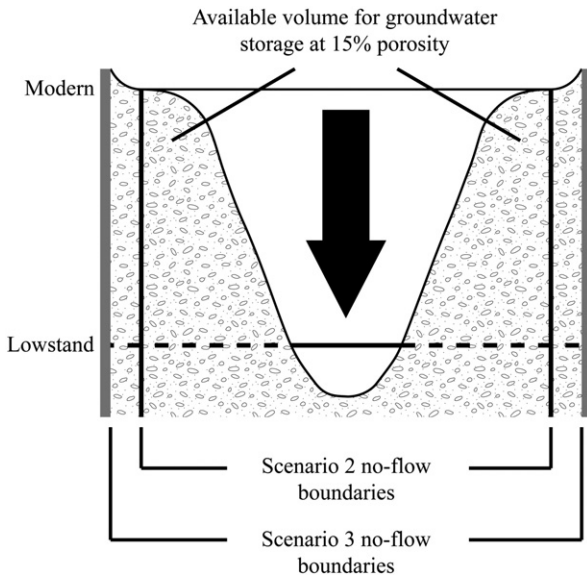


Fig. 9. Conceptual models used when accounting for groundwater storage for estimating Malawi lake-level response time; the volume of available groundwater storage is estimated assuming a 15% porosity. Scenario 1 is not shown because it assumes the lake water bottom as a no-flow boundary; in other words, there is no groundwater for storage. Scenario 2: no-flow vertical boundaries at the shoreline of the lake that extend infinitely into the subsurface (in gray). Dashed lines are the upper limits of water-yielding sediment during lowstands. Scenario 3: no-flow vertical boundaries including Quaternary alluvium in direct connection to the Lake Malawi shoreline.

developed during the previous lowstand (Calder et al., 1995). The model accounts for losses due to the Shire River when lake-level is higher than 471 masl. This extra loss in the model could explain why the simulated lake-level record underestimates the historical record from 1928 to 1948 by as much as 3 m.

To understand the monthly model output on annual to decadal time scales, 12-month summations of the basin-averaged precipitation rate (P_{bas}), evaporation rate over water (E_w), potential evaporation rate over land (E_l), and the actual evaporation over land used in the model (when $P < E_l$, $P = E_l$ for each month) were computed (Fig. 12). This shows that precipitation was consistently 100–200 mm/yr lower from 1903–1935 compared to 1935–present. Potential evaporation rates over

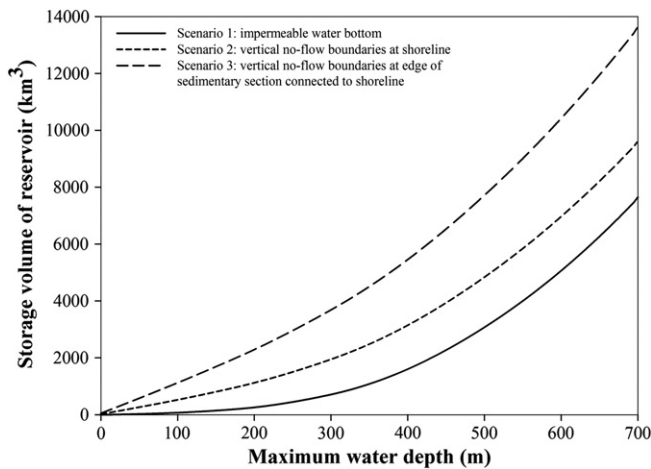


Fig. 10. Volumes of the Lake Malawi reservoir vs. maximum water depth using potential groundwater storage scenarios described in Fig. 9. Scenario 1 assumes an impermeable water bottom. This curve is the same as the cumulative volume curve from Fig. 4B. Scenario 2 assumes no-flow vertical boundaries at the shoreline of the lake with 15% porosity of storage material. Scenario 3 assumes no-flow vertical boundaries at the edge of the Quaternary alluvium and Tertiary sedimentary section that is adjacent to the lake shore.

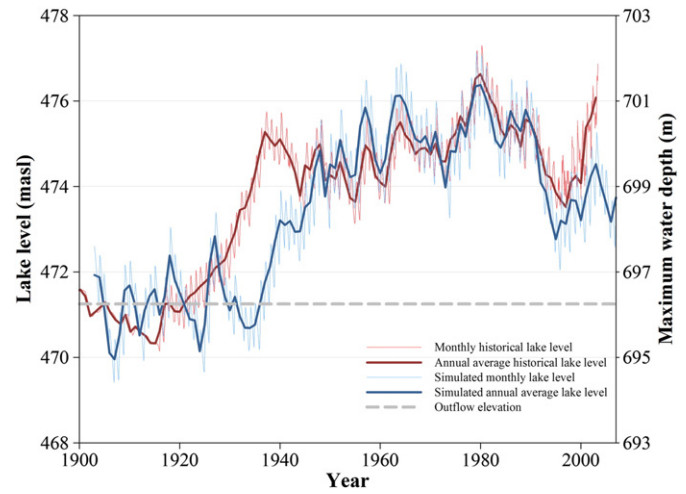


Fig. 11. Results from the historical lake-level simulation over monthly time steps. Simulated lake-level accurately predicts the historical lake-level record after 1950. Prior to 1950, sparse instrumental records used as inputs to the model and the development of sand bars across the Shire River outflow contributed to the less accurate simulation (see text for discussion).

land and water gradually increased since the first evaporation parameters were measured in 1956. The actual evaporation on land is consistently 3 times less than the potential evaporation on land. This observation plays an important role in estimating evaporation on land for the lowstand simulations, where lake-level is estimated over longer time scales.

4.2. Lowstand simulation

The balance between annual inputs (precipitation) and outputs (outflow and evaporation) of a reservoir (Lake Malawi) is expressed by a simple equilibrium equation (Eq. (14)) in terms of basin-equivalent values multiplied by their respective areas (lake area-catchment area ratios). Table 4 shows estimates of the precipitation rate required to generate equilibrium hydrologic conditions in Lake Malawi at varying lake-levels with the two sets of evaporative conditions. Modern evaporation rates over land and water were calculated from the energy-balance equations using the 1992–2007 monthly averages of relative humidity, air temperature (over

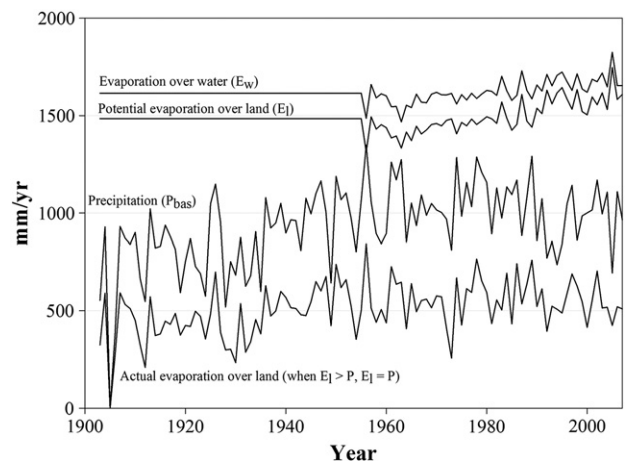


Fig. 12. Model outputs from the historical lake-level simulation. There is no climate station data available for inputs contributing to the evaporation model before 1956, so monthly averages from after 1956 were used to calculate evaporation for this interval. The discrepancy between the potential evaporation on land (E_l) and the actual evaporation on land demonstrates the importance of running the historical lake-level simulation on monthly time steps.

Table 4
Paleo-precipitation and paleo-evaporation estimates to lake-level in 50-m increments.

"Modern" conditions (using 1992–2007 average input parameters)							Best-estimate paleo-environmental lowstand conditions						
Maximum water depth (m)	a_w	E_l	E_w	O	P	Reduction from modern P (%)	Residence time (years)	E_l	E_w	P	Reduction from modern P (%)	Residence time (years)	Lowstand age (ka)
700 ^a	0.229	521	1665	172	955	100	62	N/A	N/A	N/A	N/A	N/A	Modern
696.25 ^a	0.222	521	1665	0	775	81	76	N/A	N/A	N/A	N/A	N/A	Lake closes
650	0.198	521	1665	0	747	78	65	362	1218	531	56	92	
600	0.176	521	1665	0	723	76	54	362	1218	513	54	76	
550	0.155	521	1665	0	698	73	44	362	1218	494	52	62	
500 ^b	0.133	521	1665	0	674	71	35	362	1218	476	50	50	~63
450	0.112	521	1665	0	649	68	27	362	1218	457	48	39	
400	0.090	521	1665	0	624	65	21	362	1218	439	46	29	
350 ^b	0.069	521	1665	0	600	63	15	362	1218	421	44	21	~75
300	0.047	521	1665	0	575	60	10	362	1218	402	42	14	
250	0.035	521	1665	0	561	59	6	362	1218	391	41	9	
200	0.023	521	1665	0	547	57	3	362	1218	381	40	5	
150 ^b	0.014	521	1665	0	537	56	2	362	1218	374	39	2	~95
100 ^c	0.009	521	1665	0	532	56	1	362	1218	370	39	1	~106

a_w is lake area-catchment area ratio, E_l is evaporation rate over land, E_w is evaporation rate over water, O is outflow rate, P is precipitation rate. Values are in mm/yr.

^a Critical lake-levels identified in the historical lake-level simulation.

^b Critical lake-levels identified from seismic-reflection profiles and dated from drill-core data (Scholz et al., 2007; Lyons et al., 2009).

^c Critical lake-level identified as a possible paleosol (Cohen et al., 2007).

land and water), and number of sunshine hours (Fig. 6, Table 1). To estimate actual evaporation on land, the potential evaporation rate output from the model is divided by 2.97, which is the average ratio between the potential and actual evaporation rate from 1992–2007 in the historical lake-level simulation (Fig. 11). This interval is selected for modern conditions because lake-level was relatively stable during this recent period (Fig. 11). The evaporation rate over water (E_w) and land (E_l) is 1665 and 521 mm/yr, respectively, for the modern evaporation scenario, and 1218 and 362 mm/yr, respectively, using the modern Little Karoo as a lowstand analogue (Table 4). The discrepancy in E_w between the two scenarios is due only to temperature, while the E_l discrepancy is due to both temperature and vegetation regime change (Tables 1 and 4).

The precipitation rate required to sustain equilibrium conditions at the modern lake-level (700 m maximum water depth, or 475 masl) is 955 mm/yr using Eq. (14) (Table 4). This result is consistent with the 1992–2007 annual average precipitation from the catchment's climate stations (955 mm/yr) (Fig. 12). In this case, the lake surface area and land surface area are set to modern conditions, $2.94 \times 10^4 \text{ km}^2$ and $9.91 \times 10^4 \text{ km}^2$, respectively (Table 3), where the outflow from the Shire River is 172 mm/yr. The residence time of the lake is calculated to be 62 years (Table 4).

The precipitation required to hydrologically close the basin (no Shire River outflow occurs at 696 m maximum water depth) is 775 mm/yr (Table 4). This value is consistent with the basin-averaged historical precipitation rate from 1911–1920 (786 mm/yr), when lake-level dropped below the Shire River sill and hydrologically closed the basin (Fig. 11). In this case, the lake surface area and land surface area are $2.85 \times 10^4 \text{ km}^2$ and 1.00^4 km^2 , respectively, and total lake volume is reduced to $7.52 \times 10^3 \text{ km}^3$, from the modern value of $7.63 \times 10^3 \text{ km}^3$ (Table 3). Residence time during this lake stage is 76 years (Table 4).

If evaporation rate over land and water are held constant at modern conditions, a precipitation rate of 537 mm/yr (a 44% reduction from modern conditions) is required to sustain equilibrium conditions at the known lowstand magnitude of 550 m BPLL (150 m maximum water depth at ~95 ka, Lyons et al., 2009; Scholz et al., 2007) (Table 4). A lake-level fall from the modern to this lowstand would result in a 94% decrease in lake surface area (from $2.94 \times 10^4 \text{ km}^2$ to $1.78 \times 10^3 \text{ km}^2$) and a 99% decrease in total lake volume (from $7.63 \times 10^3 \text{ km}^3$ to 104 km^3) (Fig. 4, Table 3). Using this scenario, the residence time in the lake during this lowstand is 1.5 years (Table 4).

Using modern vegetation and temperature across the Little Karoo Basin as an analogue to paleo-environmental conditions for Lake Malawi during lowstands (Tables 1 and 2, Fig. 8), the precipitation rate required to sustain equilibrium at low lake stages is generally 140–200 mm/yr lower than when using modern environmental conditions (Table 4). In other words, dropping the modern lake-level (700 m maximum water depth) to the minimum lowstand identified on seismic-reflection profiles (150 m maximum water depth), requires a constant precipitation rate of 374 mm/yr (a 61% drop in precipitation relative to modern conditions) (Table 4). This is due to the decrease in evaporation over land and water when using the cooler temperatures, and the more desert-like vegetation of the

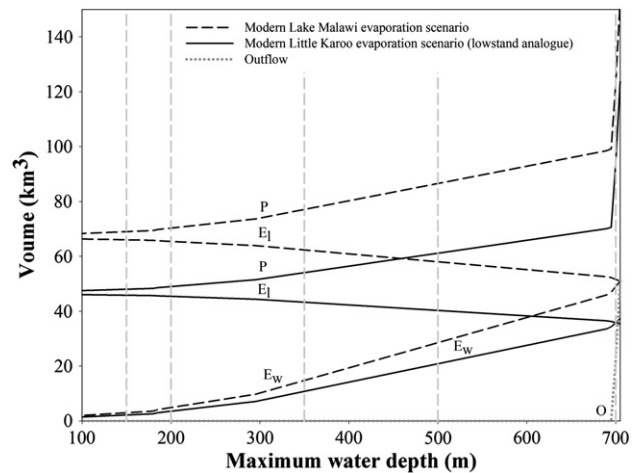


Fig. 13. Inputs and outputs required to sustain equilibrium assuming the two evaporation scenarios (Table 4), assuming both the modern Malawi vegetation and temperature and the modern Little Karoo vegetation and temperature as a Malawi lowstand analogue. Here, the volume of precipitation (P) per year required to sustain equilibrium is calculated as $P = E_w + E_l + O$, where E_w is the volume of evaporation per year over water, E_l is the volume of evaporation per year over land, and O is the volume per year of outflow. E_w and E_l are different in each scenario, and thus P varies with each. Outflow remains the same in both scenarios. The vertical dashed lines are the critical known low lake stages used in Tables 3 and 4. The effect of the outflow can be seen at water depths higher than the sill level (696 m), where all curves rise rapidly with increasing water depth.

Little Karoo Basin as input parameters to the evaporation subcomponent of the model (Fig. 8). Using this scenario, the residence time during this lowstand is 2.2 years (Table 4).

The annual precipitation required to sustain equilibrium at any given water depth is equal to the combined volume loss of the catchment due to evaporation over land, water, and loss due to outflow. A graphical computation of Eq. (14) is presented in Fig. 13, where the inputs and outputs required to sustain equilibrium conditions with varying water depth are presented in terms of volumes (km^3/yr) (Table 4). Although evaporation rate over water is always higher than over land, the total volume of water lost is always higher over land because of the larger total land area in the catchment (Fig. 13).

4.3. Response time simulation

Three sets of time-depth curves of lake-level response are presented (Fig. 14), each dropping from the modern maximum water depth (700 m) to a known low lake stage identified on seismic-reflection profiles and dated from drill-core data sets, using the three

scenarios proposed in the Methods section (Fig. 9) and with the modern Malawi evaporation scenario (Fig. 14). Each time-depth curve has an initial rapid lake-level drop, followed by a long tail that extends for 100's of years. Using an impermeable water bottom (Scenario 1) and modern evaporative conditions, less than 2500 years are required to lower lake-level from 700 m (modern) to 150 m maximum water depth (minimum lowstand), but most of the lake-level drop occurs within the first 1000 years of response time (Fig. 14a). Adding a groundwater storage component increases the response time and decreases the initial slope of lake-level drop (Fig. 14b and c). However, most of the lake-level lowering occurs within the first 1500–2000 years in both Scenarios 2 and 3, and in all cases lake-level reaches within 5 m of the final water depth within 2000 years (Fig. 14).

Refill time-depth curves from the known lowstand magnitudes to modern maximum water depth (700 m) illustrate the return to modern conditions (Fig. 14). All refill time-depth curves from all three groundwater scenarios require less than 250 years to reach 700 m water depth from their respective lowstand. Therefore, refill curves from Scenarios 2 and 3 are not included in Fig. 14.

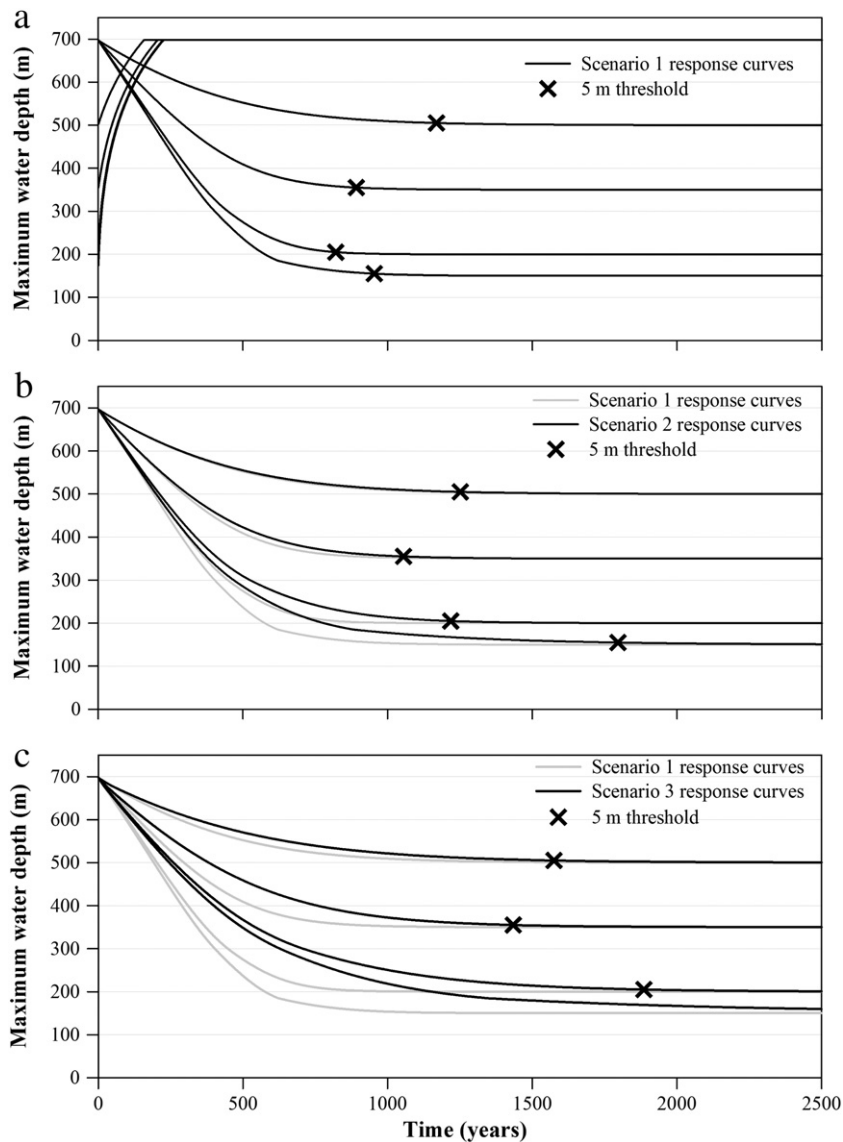


Fig. 14. Time-depth response curves using the three potential groundwater storage scenarios proposed in the text and in Fig. 9. For Scenarios 2 (b) and 3 (c), the response curves for Scenario 1 (a) are shown in grey while each equivalent response curve for Scenarios 2 and 3 are shown in black. X's mark when lake-level fall reaches within 5 m of the final water depth.

5. Discussion

5.1. Vegetation effects

Vegetation and temperature are shown to have a major effect on evaporation rate, which in turn affects the precipitation rate required to sustain equilibrium conditions during lowstands. As a Malawi lowstand analogue, the modern Little Karoo Basin vegetation and temperature were used as input parameters for the evaporation subcomponent of the energy-balance model (Fig. 8). This basin has similar topographic relief to the Malawi catchment, and a similar vegetation regime and range in mean annual air temperature (Fig. 8) to the Malawi lowstand paleo-environment (Cohen et al., 2007). The precipitation rate required to sustain equilibrium at the minimum known lowstand magnitude (150 m maximum water depth) is 374 mm/yr using the modern Little Karoo temperature and vegetation as an evaporative lowstand analogue (Table 4). This value is 163 mm/yr lower than the precipitation rate estimate (537 mm/yr) for the same lowstand when using modern Malawi vegetation and temperature. Precipitation maps of the Little Karoo Basin show between 100 and 700 mm of annual rainfall in the basin, but most of the basin receives 300–500 mm/yr (Kleynhans et al., 2005). The precipitation rate calculated here using this lowstand analogue is well within the range of annual precipitation measurements from the Little Karoo Basin and is consistent with interpretations from Lake Malawi drill-core data sets (Cohen et al., 2007), where the absence of charred particles in the drill-core during lowstands suggests a precipitation rate of less than 400 mm/yr, the threshold for fire-sustaining fuel beds (Bird et al., 2004). This demonstrates the importance of understanding past vegetation regimes and paleo-temperatures, parameters that can only be estimated from paleoclimate data sets. Unlike this study, several previous studies did not have access to such data sets to estimate these effects (e.g. Bergonzini et al., 1997; Bookhagen et al., 2001).

To generate severe low lake-levels, it is possible to increase evaporation rather than decrease precipitation. However, all parameters (temperature, soil moisture, surface emissivity, albedo, and roughness length) used from the Little Karoo lowstand analogue reduce evaporation (Fig. 8; Table 2). The reduced soil moisture, roughness length, surface emissivity, and increased albedo as a result of the more desert-like conditions (indicated by beige colors in Fig. 8, Table 2), and 5–7 °C cooler temperatures of the Little Karoo deter evaporation during lowstand intervals, thus decreasing the precipitation rate required to sustain equilibrium at known lowstand magnitudes (Fig. 8). Accordingly, reducing precipitation rate is the only realistic mechanism for inducing the major drops in lake-level documented from paleoclimate data sets (Cohen et al., 2007; Scholz et al., 2007; Lyons et al., 2009), while concurrently decreasing evaporation rate (required due to cooler temperature and vegetation change) during lowstands (Table 4).

5.2. Lowstand simulation

Evaporation over land (E_l) is always higher than over water (E_w) when plotted in terms of volumes, and increases as maximum water depth decreases (Fig. 13). This is due to the decrease in lake surface area (land surface area increasing) as maximum water depth decreases. Even though the evaporation rate (per unit area) over water is always higher than over land, land area is always greater than lake surface area, and thus the volume loss from the basin is always more from the land. Furthermore, as maximum water depth decreases, there is an increasing proportion of water that is lost before it enters the lake. This is due to an increase in overland transport as the lake surface area decreases. Also, the impact of the Shire River outflow on the hydrologic balance of the system is considerable (see Fig. 13), and illustrates why the maximum highstand has been at or just above the sill elevation. The precipitation and evaporation rates required to

sustain equilibrium dramatically increase above 696 m water depth, which is the sill elevation (Table 3).

As mentioned in the results, the average ratio between the annual potential evaporation rate and actual evaporation rate over land was 2.97 in the historical lake-level simulation (Fig. 12). This discrepancy is due to the wet-dry seasonal cycle of the Lake Malawi catchment, and can only be calculated using a sub-annual modeling routine. If potential evaporation rate over land was used in the lowstand and response time simulation routines, the precipitation rate required to sustain equilibrium during lowstands would have been overestimated (Fig. 12). Therefore, by using a monthly time step in the historical lake-level simulation, we accurately capture seasonal variations in the available water to evaporate on land and gain an understanding of the relationship of potential and actual evaporation. Thus, this demonstrates the superiority of using a monthly time step for simulation over historical time scales.

Lower lake stages decrease the water residence time of the basin (Table 4), and indicate the increasing sensitivity of the lake as maximum water depth decreases. The highest residence time is at the basin closure (76 years) while at maximum water depth (700 m), the residence time is 62 years (Table 4), due to the Shire River outflow. A similar trend is observed in the precipitation rate required to sustain equilibrium at critical known lake-levels (Table 4). A 180 mm/yr drop in precipitation rate (955 to 775 mm/yr) is required to close the basin from modern levels (4 m drop in lake-level). An additional 238 or 401 mm/yr drop in precipitation rate (from 775 to 537 or 374 mm/yr) using modern Malawi vegetation and temperature or Little Karoo vegetation and temperature, is required to drop lake-level to a 150 m maximum water depth (Tables 3 and 4) (Lyons et al., 2009). These values demonstrate that the lake is much less sensitive to hydrologic change when the outflow is present.

5.3. Response time simulation

Each set of time-depth response curves demonstrates an initial rapid response followed by a long extended tail (Fig. 14). In the model, the shapes of these curves are due to the relationship between lake surface area and evaporation from that surface. An instantaneous drop in precipitation from modern conditions produces a disequilibrium system where the expansive lake loses volume rapidly through both the outflow and from direct evaporation from its surface. This results in the rapid drop in lake-level observed in the time-depth curves (Fig. 14). As the system progresses towards equilibrium, the basin closes and lake surface area decreases, thus reducing direct water loss from the system, resulting in a less rapid fall as observed on the time-depth curves (Fig. 14). The faster refill response times are a result of the presence of outflow from the Shire River (Fig. 13). If this outflow is not present, lake-level continues to rise in a similar extended fashion to the time-depth curves of the lake-level drops (Fig. 14). In other words, the presence of an outflow dramatically increases the precipitation required to sustain equilibrium conditions above 696 m maximum water depth.

The additional groundwater component used in Scenarios 2 and 3 increases the storage size of the reservoir (Fig. 9). This increases the water volume loss (gain) required to drop (raise) lake-level for every time step during the response simulation (Fig. 14). This effect has the largest impact when lake-level is between 190 m and 300 m water depth, where the change in volume per depth is significantly higher in Scenarios 2 and 3 relative to Scenario 1 (Fig. 14). Therefore, when assessing lake-level fall, the initial response observed in Scenario 1 (no groundwater storage component) is more rapid than in Scenarios 2 and 3 (additional groundwater storage components) until 190 m maximum water depth is reached (Fig. 14). However, as lake-level continues to fall, the difference in the total size of the reservoirs in each scenario decreases. Therefore, by 2000 years of response time, the time-depth curves in each scenario all reach similar lake-levels (Fig. 14).

5.4. Paleoclimate implications and facies development

Changes in insolation on orbital precession time scales can affect the intensity and duration of the wet (monsoon) season over Lake Malawi, especially during intervals of high orbital eccentricity (Scholz et al., 2007). Intervals of megadrought correlate to insolation minima at the precession frequency (~20,000 years) during the beginning of the rainy season (October to December). Scholz et al. (2007) argue that a reduction in the duration and/or intensity of the rainy season, via changes in ITCZ position and intensity, induces the well-documented lowstands. Therefore, we argue that insolation forcing occurs through this “regional filter” and water balance locally within the Lake Malawi catchment is a combined effect of local forcing as well as variability in the ITCZ. Greater than 85% of the total rainfall in the Lake Malawi catchment occurs from December to April (Fig. 3). A reduction in precipitation rate from 955 mm/yr to 374 mm/yr is required to induce the lake-level fall suggested by Scholz et al. (2007) (Table 4), while also accounting for major changes in major temperature and vegetation regime. Such a dramatic reduction in the annual precipitation across the Lake Malawi catchment must have occurred primarily during the wet season to have had such a major impact on the hydrologic budget (Fig. 2).

Casteñeda et al. (2007) argue that vegetation change can occur even on sub-orbital time scales in the Lake Malawi catchment, and that it is primarily driven by aridity, rather than temperature. This change sets up a negative feedback system, where an insolation minimum reduces the duration and/or intensity of tropical convergence and thus reduces the duration and/or intensity of the austral monsoon season (Scholz et al., 2007). Such aridity causes a negative water balance in the Lake Malawi system, resulting in lake-level fall (Fig. 14). Aridity also causes a vegetation transition to a semi-desert environment (Cohen et al., 2007; Beuning et al., 2010), which in conjunction with cooler temperatures limits evaporation, thus requiring a further reduction in precipitation to generate continued lake-level fall (Table 4, Fig. 10).

Using water balance calculations, Owen et al. (1990) estimated time-depth curves for Lake Malawi, where a 50% decrease in precipitation rate would cause a 500 m drop in lake-level from the modern lake stage (700 m) over 600 years. For the same lowstand level, a 43% drop in precipitation is observed in this model when assuming modern vegetation and temperature, and a 60% precipitation drop is required when assuming vegetation and temperature comparable to the Little Karoo Basin (Table 4). The response times of lake-level estimated here are between 1000 and 2000 years. This discrepancy with Owen et al. (1990) in response time does not discount the findings of the authors, because their lake-level curve slopes are similar in shape to those generated here, with initial rapid lake-level fall followed by an extended tail. However, the limited bathymetric data available in Owen et al. (1990), especially in deep water, may have contributed to the geometry of their curves. Using an extensive set of seismic-reflection data, superior bathymetry was generated for this study, especially in deep water, which results in more accurate hypsometric and cumulative volume curves (Fig. 4).

Bootsma and Hecky (1993) report a modern residence time for Lake Malawi of 140 years, 80 years greater than calculated here (Table 4). They calculated this value based on a total volume reported by Gonfiantini et al. (1979) and precipitation volume input calculated by Owen et al. (1990). However, cumulative volume calculated here is based on the superior bathymetric data set (Lyons et al., 2009), and precipitation volume input is based on all of the available climate station data within the Lake Malawi catchment.

The time-depth curves presented here (Fig. 14) are consistent with the lake-level interpretations from Scholz et al. (2007) and Lyons et al. (2009). They suggest that Malawi lake-level initially responds quickly to changing atmospheric conditions. There is limited evidence for transgressive and regressive facies in both drill-core data and seismic-

reflection data, suggesting rapid lake-level change during transitional intervals (Scholz et al., 2007; Cohen et al., 2007; Lyons et al., 2009). The rapid lake-level response observed in the time-depth curves (Fig. 14) and lower residence times during lowstands (Table 4) may be the primary reason for the general absence of transgressive and regressive facies observed in the lake (Lyons et al., 2009).

6. Summary and conclusions

Based on the numerical simulations performed in this study, the following conclusions can be drawn:

- (1) The Lake Malawi historical lake-level record is successfully simulated since 1950 using an energy-balance hydrologic model. Before 1950, the simulation breaks down due to the lack of instrumental data used for input into the model. The development of sand bars when the Shire River outflow closed may have contributed to the model's underestimation of lake-level during transgression before 1950.
- (2) Using outputs from these historical lake-level simulations, the precipitation rate required to sustain equilibrium conditions at 50-m intervals is estimated. Using this steady-state system, the modern estimate of 955 mm/yr and lake closure estimate of 775 mm/yr precipitation rate is consistent with modern and lake closure precipitation rates observed in the historical simulation. The precipitation rate required to sustain equilibrium at the minimum known low lake stage identified in seismic-reflection profiles (150 m maximum water depth) is 537 mm/yr (44% lower than modern) using modern Malawi evaporation conditions and 374 mm/yr (61% lower than modern) using a modern catchment basin (Little Karoo) that has evaporative conditions analogous to the Malawi Rift valley during the megadrought and severe lowstand intervals. These results are consistent with both the modern precipitation from the Little Karoo Basin and interpretations from Lake Malawi drill-core data sets (Cohen et al., 2007), and demonstrate the impact that temperature and vegetation regime change can have on a hydrologic system.
- (3) Lake-level fall occurs within the first 1000 years when applying paleoprecipitation estimates to the modern system. Even when accounting for changes in potential groundwater storage, almost all of the lake-level fall occurs within 2500 years. Refill occurs within 250 years, even following the most severe draw-down. These results suggest the hydrologic system can respond quickly to changing atmospheric conditions. The potential for rapid lake-level response simulated here may explain the lack of transgressive and regressive facies observed in Lake Malawi seismic-reflection data and drill-core data.
- (4) These results suggest a negative feedback system in the Lake Malawi catchment, where aridity causes lake-level fall and a change in the vegetation regime of the catchment. Cooler temperatures and vegetation change both reduce evaporation, thus requiring an even greater reduction in precipitation to achieve further fall in lake-level.

References

- Anselmetti, F.S., Ariztegui, D., De Batist, M., Gebhardt, A.C., Haberzettl, T., Niessen, F., Ohlendorf, C., Zolitschka, B., 2009. Environmental history of southern Patagonia unravelled by the seismic stratigraphy of Laguna Potrok Aike. *Sedimentology* 56, 873–892.
- Bergner, A.G.N., Trauth, M.H., Bookhagen, B., 2003. Paleoprecipitation estimates for the Lake Naivasha basin (Kenya) during the last 175 k.y. using a lake-balance model. *Global and Planetary Change* 36, 117–136.
- Bergonzini, L., Chalif, F., Gasse, F., 1997. Paleoevaporation and paleoprecipitation in the Tanganyika basin at 18,000 years B.P. inferred from hydrologic and vegetation proxies.
- Beuning, K.R.M., Zimmerman, K.A., Ivory, S.J., Cohen, A.S., 2010. Vegetation response to glacial-interglacial climate variability near Lake Malawi in the southern African tropics. *Palaeogeography, Palaeoclimatology, Palaeoecology*.

- Bird, M.I., Veenendaal, M., Lloyd, J.J., 2004. Soil carbon inventories and $\delta^{13}\text{C}$ along a moisture gradient in Botswana. *Global Change Biology* 10, 342–349.
- Blodgett, T.A., Lenters, J.D., Isacks, B.L., 1997. Constraints on the origin of paleolake expansions in the central Andes. *Earth Interactions* 1 (1), 1–28.
- Bookhagen, B., Haselton, K., Trauth, M.H., 2001. Hydrologic modelling of a Pleistocene landslide-dammed lake in the Santa Maria Basin, Argentina. *Palaeogeography, Palaeoclimatology, Palaeoecology* 169, 113–127.
- Bootsma, H.A., Hecky, R.E., 1993. Conservation of the African Great Lakes: a limnological perspective. *Conservation Biology* 7 (3), 644–656.
- Bougealt, P., 1991. Parameterization of land surface processes in numerical weather prediction. In: Schmugge, T.J., Andre, J.C. (Eds.), *Land Surface Evaporation: Measurement and Parameterization*. Springer-Verlag, New York, pp. 55–92.
- Brooks, K., Scholz, C.A., King, J.W., Peck, J., Overpeck, J.T., Russell, J.M., Amoako, P.Y.O., 2005. Late-Quaternary lowstands of lake Bosumtwi, Ghana: evidence from high-resolution seismic-reflection and sediment-core data. *Palaeogeography, Palaeoclimatology, Palaeoecology* 216 (3–4), 235–249.
- Brutsaert, W.H., 1982. *Evaporation into the Atmosphere: Theory, History, Applications*. D. Reidel Publishing, Dordrecht, 299 pgs.
- Budyko, M.I., 1974. *Climate and Life*. International Geophysics Series, 18. Academic Press, New York.
- Buoniconti, M.R., 2000. The sequence stratigraphy of the Songwe delta, a rift lake axial margin delta, Lake Malawi, East Africa. Masters Thesis, University of Miami.
- Calder, I.R., Hall, R.L., Bastable, H.G., Gunston, H.M., Osborne, S., Chirwa, A., Kafundu, R., 1995. The impact of land use change on water resources in sub-Saharan Africa: a modelling study of Lake Malawi. *Journal of Hydrology* 170, 123–135.
- Casteñeda, I.S., Werne, J.P., Johnson, T.C., 2007. Wet and arid phases in southeast African tropics since the Last Glacial Maximum. *Geology* 9, 823–826.
- Cohen, A.S., Stone, J.R., Beuning, K.R.M., Park, L.E., Reinthal, P.N., Dettman, D., Scholz, C.A., Johnson, T.C., King, J.W., Talbot, M.R., Brown, E.T., Ivory, S.J., 2007. Ecological Consequences of Early Late Pleistocene Megadroughts in Tropical Africa. *Proceedings of the National Academy of Sciences* 104 (42), 16422–16427.
- Conroy, J.L., Overpeck, J.T., Cole, J.E., Shanahan, T.M., Steinitz-Kannan, M., 2008. Holocene changes in eastern tropical Pacific climate inferred from a Galápagos lake sediment record. *Quaternary Science Reviews* 27, 1166–1180.
- D'Agostino, K., Seltzer, G., Baker, P., Fritz, S., Dunbar, R., 2002. Late-Quaternary lowstands of Lake Titicaca: evidence from high-resolution seismic data. *Palaeogeography, Palaeoclimatology, Palaeoecology* 179, 93–111.
- Desmet, P.G., Cowling, R.M., 1999. The climate of the Karoo—a functional approach. In: Dean, W.R.J., Milton, S.J. (Eds.), *The Karoo: ecological patterns and processes*. Cambridge University Press, pp. 3–16.
- Drayton, R.S., 1984. Variations in the level of Lake Malawi. *Hydrologic Sciences* 29, 1–12.
- Gonfiantini, R., Zuppi, G.M., Eccles, D.H., Ferro, W., 1979. Isotope Investigation of Lake Malawi. *Isotopes in Lake Studies*. International Atomic Energy Agency, Vienna, Austria, pp. 195–207.
- Hastenrath, S., Kutzbach, J.E., 1983. Paleoclimatic estimates from water and energy budgets of East African Lakes. *Quaternary Research* 19, 141–153.
- Kidd, C.H.R., 1983. A water resources evaluation of Lake Malawi and the Shire River. UNDP project report MLW/77/012. 135 pgs.
- Kingdon, M.J., Bootsma, H.A., Mwitwa, J., Mwichande, B., Hecky, R.E., 1999. River Discharge and Water Quality. In: Bootsma, H.A., Hecky, R.E. (Eds.), *Water Quality Report. Lake Malawi/Nyasa biodiversity conservation project*, Malawi, pp. 29–69.
- Kleynhans, C.J., Thirion, C., Moolman, J., 2005. A level I river ecoregion classification system for South Africa, Lesotho and Swaziland. Report No. N/0000/00/REQ0104. Resource Quality Services, Department of Water Affairs and Forestry, Pretoria, South Africa. 78 pgs.
- Laskar, J., Robutel, P., Joutel, F., Gastineau, M., Correia, A.C.M., Levrard, B., 2004. A long-term numerical solution for the insolation quantities of the Earth. *Astronomy & Astrophysics* 428 (1), 261–285.
- Lyons, R.P., Scholz, C.A., Buoniconti, M.R., Martin, M.R., 2009. Late Quaternary stratigraphic analysis of the Lake Malawi Rift: East Africa: an integration of drill-core and seismic-reflection data. *Palaeogeography, Palaeoclimatology, Palaeoecology*.
- Malawi Department of Surveys, 1983. *National Atlas of Malawi*: Blantyre, Malawi. 79 pgs.
- Martin, M.R., 1997. The sequence stratigraphy of a rift lake flexural margin delta: Dwangwa delta, Lake Malawi, East Africa. Masters Thesis, University of Houston.
- McGlue, M.M., Scholz, C.A., Karp, T., Ongodia, B., Lezzar, K.E., 2006. Facies architecture of flexural margin lowstand delta deposits in Lake Edward, East African Rift: constraints from seismic reflection imaging. *Journal of Sedimentary Research* 76, 942–958.
- Mozambique Ministry of Mineral Resources, 1987. *Geologic Map*. Republic of Mozambique.
- Nicholson, S.E., 2000. The nature of rainfall variability over Africa on time scales of decades to millennia. *Global and Planetary Change* 26, 137–158.
- Owen, R.B., Crossley, R., Johnson, T.C., Tweddle, D., Kornfield, I., Davison, S., Eccles, D.H., Engstrom, D.E., 1990. Major low lake levels of Lake Malawi and their implications for speciation rates in cichlid fishes. *Proceedings of the Royal Society of London. Series B, Biological Sciences* B240, 519–553.
- Rowe, H.D., Dunbar, R.B., 2004. Hydrologic-energy balance constraints on the Holocene lake-level history of Lake Titicaca, South America. *Climate Dynamics* 23, 439–454.
- Russell, J.M., Johnson, T.C., 2007. Little Ice Age drought in equatorial Africa: intertropical convergence zone migration and El Niño–Southern Oscillation variability. *Geology* 35 (1), 21–24.
- Scholz, C.A., King, J.W., Ellis, G.S., Swart, P.K., Stager, J.C., Colman, S.M., 2003. Paleolimnology of Lake Tanganyika, East Africa, over the past 100 kyr. *Journal of Paleolimnology* 30, 139–150.
- Scholz, C.A., Johnson, T.C., Cohen, A.C., King, J.W., Peck, J.A., Overpeck, J.T., Talbot, M.R., Brown, E.T., Kalindekafu, L., Amoako, P.Y.O., Lyons, R.P., Shanahan, T.M., Castaneda, I.S., Heil, C.W., Forman, S.L., McHargue, L.R., Beuning, K.R., Gomez, J., Pierson, J., 2007. East African megadroughts between 135 and 75 thousand years ago and bearing on early-modern human origins. *Proceedings of the National Academy of Sciences* 104 (42), 16416–16421.
- Schwartz, F.W., Zhang, H., 2002. *Fundamentals of Ground Water*. John Wiley and Sons, Inc. 583 pgs.
- Shanahan, T.M., Overpeck, J.T., Sharp, W.E., Scholz, C.A., Arko, J.A., 2007. Simulating the response of a closed-basin lake to recent climate changes in tropical West Africa (Lake Bosumtwi, Ghana). *Hydrologic Processes* 21, 1678–1691.
- Shanahan, T.M., Overpeck, J.T., Anchukaitis, K.J., Beck, J.W., Cole, J.E., Dettman, D.L., Peck, J.A., Scholz, C.A., King, J.W., 2009. Atlantic forcing of persistent drought in West Africa. *Science* 324 (5925), 377–380.
- Smith-Carrington, A.K., Chilton, P.J., 1983. *The Groundwater Resources of Malawi*. Malawi Government report, Lilongwe.
- Soreghan, M.J., Scholz, C.A., Wells, J.T., 1999. Coarse-grained, deep-water sedimentation along a border fault margin of Lake Malawi, Africa: seismic stratigraphic analysis. *Journal of Sedimentary Research* 69 (4), 832–846.
- Specht, T.D., Rosendahl, B.R., 1989. Architecture of the Lake Malawi Rift, East Africa. In: Rogers, J.J.W., Rach, N.M. (Eds.), *Journal of African Earth Sciences Special Issue, Africa Rifting* 8. Elsevier, London, pp. 355–382.
- Trauth, M.H., Deino, A.L., Bergner, A.G.N., Strecker, M.R., 2003. East African climate change and orbital forcing during the last 175 kyr BP. *Earth and Planetary Science Letters* 206 (3–4), 297–313.
- Vallet-Coloumb, C., Gasse, F., Sonzogni, C., 2008. Seasonal evolution of the isotopic composition of atmospheric water vapour above a tropical lake: deuterium excess and implication for water recycling. *Geochimica et Cosmochimica Acta* 72 (18), 4661–4674.
- Vollmer, M.K., Bootsma, H.A., Hecky, R.E., Patterson, G., Halfman, J.D., Edmond, J.M., Eccles, D.H., Weiss, R.F., 2005. Deep-water warming trend in Lake Malawi, East Africa. *Limnology and Oceanography* 50 (2), 727–732.
- Woltering, M., Johnson, T.C., Werne, J.P., Schouten, S., in press. Late Pleistocene temperature history of Southeast Africa: A TEX₈₆ temperature record from Lake Malawi. *Palaeogeography, Palaeoclimatology, Palaeoecology*. doi:10.1016/j.palaeo.2010.02.013
- Yin, X., Nicholson, S.E., 1998. The water balance of Lake Victoria. *Hydrologic Sciences Journal* 43 (5), 789–811.